

Crosstalk Spectrum Predictions Considering Frequency-Dependent Parameters in Electric Vehicles

Yanjie Guo, Lifang Wang, and Chenglin Liao

Key Laboratory of Power Electronics and Electric Drive
Institute of Electrical Engineering, Chinese Academy of Sciences
No.6 Beiertiao, Zhongguancun, Beijing, 100190, China
yjguo@mail.iee.ac.cn, wlf@mail.iee.ac.cn, liaocl@mail.iee.ac.cn

Abstract — This paper presents a method which combines impedance measurements, calculations, and equivalent model together to predict crosstalk spectrums. It is simple for calculation and also has good accuracy, because frequency-dependent parameters of both cables and terminal loads are considered. So it has advantages in some complex situations such as electric vehicle (EV). Firstly, a model of single line and twisted-pair wires is established to describe the crosstalk system. In this model, crosstalk voltage expressions are given, and frequency-dependent parameters are obtained from impedance measurements and calculations. Then in order to verify the method, crosstalk spectrums are predicted under conditions of resistance load and frequency-dependent load. Furthermore, predictions and experiments are compared to assess the effectiveness of the method. Based on the predicted and experimental results, frequency domain characteristics of crosstalk are discussed and influence factors are analyzed.

Index Terms — Crosstalk, electromagnetic compatibility, frequency domain analysis, frequency estimation, impedance measurement.

I. INTRODUCTION

Crosstalk problems appear in many integrated electric or electrical systems [1]. Crosstalk among cables is the main interference propagation path when cables are banded together or placed closely [2]. High power interference sources and restricted spaces in electric vehicle (EV) make it even worse. Bus-connected units are usually vulnerable to these crosstalk interferences, which decline the stability and safety of the entire vehicle.

Some research on the transmission line can help to analyze this problem [3-6]. Also, the distributed parameters are used to analyze cables in the frequency domain or the complex frequency domain; for example, finite difference time domain (FDTD) [7,8] and methods of moments [9]. However, under some complicated conditions, such as EV applications, these methods are

not applicable because long simulation time and massive computing resources are required. Another method is lumped parameter descriptions [10,11]. But this method ignores the distributed parameters which affect the high frequency characteristics significantly. Furthermore, communication systems, such as controller area network (CAN) buses, have been tested to estimate the impacts of electromagnetic interferences [12]. Moreover, attempts of taking statistical results as input signals have been experimented to get crosstalk waveforms [13]. Though these methods can represent some interference characteristics clearly, they are not related to the mechanism of the crosstalk system and do little help to solve the problem fundamentally.

To the twisted-pair wires which are widely used in communication buses in EV, the typical method is to treat them as spiral lines, get distributed parameters of one twist and integrate all twists to parameter matrixes [14]. This will lead to substantial calculations and inaccuracy under the EV environment, where frequency-dependent parameters commonly exist.

Developments of impedance measurement technology provide a way to get frequency-dependent parameters [15-17]. Frequency-dependent parameters can be obtained from open-circuit and short-circuit impedance measurements. This technology can be extended to crosstalk analysis to obtain the frequency-dependent parameters of crosstalk systems. With the crosstalk equivalent model together, it can be used to predict the crosstalk interference spectrums.

The above discussions suggest traditional crosstalk calculation methods have limits in some complex situations, such as EV applications because of the following reasons: length of the cable is not meet the requirement of electric short; conductors and non-uniform dielectric objects around make non-uniform distributions of charge and flux in the cable; skin effect and proximity effect in high frequency range; irregular cable shape and inconsistent distances between cables, etc. These factors will significantly increase the calculation and bring the deviation.

So in this paper, we used cable parameters calculated from actual measurement results to make sure the above factors are considered. Furthermore, we established an approximate lumped parameter crosstalk model. Combined with the model and the frequency-dependent parameters, we proposed a crosstalk prediction method. It is simple for calculation because of the lumped parameters model. Also, it has good accuracy because the frequency-dependent parameters obtained from measurements are considered. At last, the proposed method is verified on conditions of both resistance load and frequency-dependent load.

II. SPECTRUM PREDICTION METHOD

The spectrum prediction method contains two stages: one is the crosstalk model expressing the cable system; the other is the impedance measurements and calculations from which frequency-dependent parameters of the crosstalk model obtain. To predict the spectrums, firstly, the input impedances among cables and the impedances of terminal loads are measured. Then, the frequency-dependent parameters of the crosstalk system are calculated. Finally, the parameters are taken into the frequency domain expressions which are obtained from the crosstalk model to get the crosstalk voltage spectrums.

A. Equivalent model

Figure 1 shows the equivalent model of single line and twisted-pair wires which is used to analyze crosstalk among cables in EV. The purpose of crosstalk analysis in this paper is to define the spectrums of the voltage on the near terminal $U_{11}(j\omega)$ and the voltage on the remote terminal $U_{12}(j\omega)$.

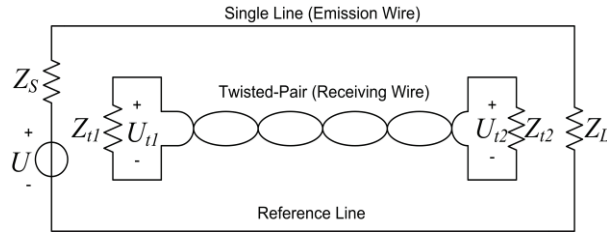


Fig. 1. Equivalent model of crosstalk system containing single line and twisted-pair wires.

Firstly, effect of twisted-pair wires on single line is approximately expressed in order to get the current and voltage in the single line. Because the inductive coupling between single line and twisted-pair wires is proportional to the difference of mutual-inductances between single line and the two twisted-pair wires; hence, an inductance L_{sf} is introduced to show twisted-pair wires' effect as shown in Fig. 2. And its value is approximately given by equation (1):

$$L_{sf} \approx L_s + \alpha(M_{st1} - M_{st2}), \quad (1)$$

where L_s is the self-inductance of the single line; M_{st1} and M_{st2} are mutual-inductances between single line and twisted-pair wires; α is the coefficient related to the difference of power levels between single line and twisted-pair wires. Also, R_{sf} is used to express the resistance of the single line, which is frequency-dependent because of the skin effects.

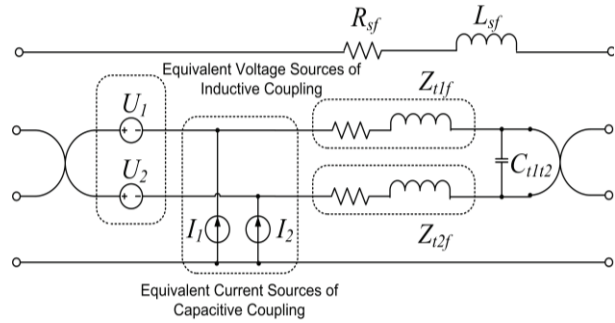


Fig. 2. Equivalent parameters and inductive, capacitive coupling equivalent sources.

So the current and voltage in single line are defined by equation (2):

$$I_s(j\omega) = \frac{U(j\omega)}{Z_s(j\omega) + Z_L(j\omega) + R_{sf}(j\omega) + j\omega L_{sf}(j\omega)}, \quad (2)$$

$$U_s(j\omega) = \frac{Z_L(j\omega)U(j\omega)}{Z_s(j\omega) + Z_L(j\omega) + R_{sf}(j\omega) + j\omega L_{sf}(j\omega)}.$$

Then treating $U_s(j\omega)$ and $I_s(j\omega)$ as interference sources, effects of inductive and capacitive couplings can be equivalent to voltage and current sources given by equation (3) [18] and shown in Fig. 2:

$$\begin{aligned} U_1(j\omega) &= M_{st1}j\omega I_s(j\omega), \\ U_2(j\omega) &= M_{st2}j\omega I_s(j\omega), \\ I_1(j\omega) &= C_{st1}j\omega U_s(j\omega), \\ I_2(j\omega) &= C_{st2}j\omega U_s(j\omega), \end{aligned} \quad (3)$$

where C_{st1} and C_{st2} are coupling capacitances between the single line and the two twisted-pair wires.

Finally, crosstalk voltages on the near and the remote terminal are calculated. And their frequency domain forms are given by equation (4) and equation (5). Where,

$$\begin{aligned} U_{11}(j\omega) &= \left(\frac{Z_{11}(j\omega)}{Z_{11}(j\omega) + Z_{12}(j\omega) + Z_{11f}(j\omega) + Z_{12f}(j\omega)} \right) \\ &\quad \times (U_1(j\omega) - U_2(j\omega)) \\ &\quad + \frac{Z_{11}(j\omega)(Z_{12}(j\omega) // C_{112} + Z_{11f}(j\omega) + Z_{12f}(j\omega))}{Z_{11}(j\omega) + Z_{12}(j\omega) // C_{112} + Z_{11f}(j\omega) + Z_{12f}(j\omega)} \\ &\quad \times \frac{Z_{11}(j\omega)}{Z_{11}(j\omega) + Z_{11f}(j\omega) + Z_{12f}(j\omega)} \\ &\quad \times (I_1(j\omega) + I_2(j\omega)). \end{aligned} \quad (4)$$

$$\begin{aligned}
 U_{i2}(j\omega) = & \left(-\frac{Z_{i2}(j\omega)}{Z_{i1}(j\omega) + Z_{i2}(j\omega) + Z_{i1f}(j\omega) + Z_{i2f}(j\omega)} \right. \\
 & \times (U_1(j\omega) - U_2(j\omega)) \\
 & + \frac{Z_{i1}(j\omega)(Z_{i2}(j\omega) / C_{i1i2} + Z_{i1f}(j\omega) + Z_{i2f}(j\omega))}{Z_{i1}(j\omega) + Z_{i2}(j\omega) / C_{i1i2} + Z_{i1f}(j\omega) + Z_{i2f}(j\omega)} \\
 & \times \frac{Z_{i2}(j\omega) / C_{i1i2}}{Z_{i2}(j\omega) / C_{i1i2} + Z_{i1f}(j\omega) + Z_{i2f}(j\omega)} \\
 & \left. \times (I_1(j\omega) + I_2(j\omega)) \right). \quad (5)
 \end{aligned}$$

“/” means the two impedance variables are in parallel; Z_{i1f} and Z_{i2f} are the equivalent self-impedances of the twisted-pair wires, which contain the self-resistances, self-inductances of the twisted-pair wires.

B. Frequency-dependent parameter calculation

Equation (4) and (5) indicate that there are two kinds of frequency-dependent parameters. One is terminal loads, such as Z_s , Z_L , Z_{i1} , and Z_{i2} . The other is the parameters of the cables, including the equivalent impedances L_{sf} , Z_{i1f} , Z_{i2f} ; mutual inductances M_{st1} , M_{st2} and coupling capacitances C_{st1} , C_{st2} , C_{i1i2} . The former can be directly measured by an impedance analyzer. The latter can be calculated through the following steps.

Firstly, the elements of impedance matrixes Z_{sc} and Z_{oc} can be expressed by input measurement impedances as follows:

$$\begin{aligned}
 Z_{sc}(i, i) &= Z_{in}^{sc}(i, i), \\
 Z_{sc}(i, j) &= [Z_{in}^{sc}(i, i) + Z_{in}^{sc}(j, j) - Z_{in}^{sc}(i, j)] / 2, \quad (6) \\
 Z_{oc}(i, i) &= Z_{in}^{oc}(i, i), \\
 Z_{oc}(i, j) &= [Z_{in}^{oc}(i, i) + Z_{in}^{oc}(j, j) - Z_{in}^{oc}(i, j)] / 2,
 \end{aligned}$$

where $Z_{sc}(i, i)$, $Z_{sc}(i, j)$ and $Z_{oc}(i, i)$, $Z_{oc}(i, j)$ are diagonal, non-diagonal elements of the short-circuit impedance matrix Z_{sc} and the open-circuit impedance matrix Z_{oc} ; $Z_{in}^{sc}(i, i)$ and $Z_{in}^{oc}(i, i)$ are short-circuit and open-circuit input measurement impedances between conductor i and the reference conductor; $Z_{in}^{sc}(i, j)$ and $Z_{in}^{oc}(i, j)$ are short-circuit and open-circuit input measurement impedances between conductor i and conductor j ; $i, j = 1, 2, \dots, N$ and $i \neq j$, N is the number of the conductors.

Then, series impedance matrix Z and parallel admittance matrix Y are obtained from Z_{sc} and Z_{oc} through equation (7). Where l is the lengths of the cables; Γ and Z_c are the propagation constant matrix and the characteristic impedance matrix:

$$\begin{aligned}
 \Gamma &= \arctan h \left[\left(Z_{sc} Z_{oc}^{-1} \right)^{1/2} \right] / l, \\
 Z_c &= \left(Z_{sc} Z_{oc}^{-1} \right)^{1/2} Z_{oc}, \quad (7) \\
 Z &= \Gamma Z_c, \quad Y = \left(Z_c \right)^{-1} \Gamma.
 \end{aligned}$$

Finally, frequency-dependent resistance matrix R , inductance matrix L , admittance matrix G and capacitance matrix C are given by equation (8):

$$\begin{aligned}
 R &= \text{Re}[Z(j\omega)], \quad L = \text{Im}[Z(j\omega)] / \omega, \\
 G &= \text{Re}[Y(j\omega)], \quad C = \text{Im}[Y(j\omega)] / \omega. \quad (8)
 \end{aligned}$$

So, the parameters of the cables can be found or calculated in the elements of R , G , L and C . Combining with the directly measurement results of Z_s , Z_L , Z_{i1} , and Z_{i2} , spectrums of crosstalk voltage $U_{i1}(j\omega)$ and $U_{i2}(j\omega)$ can be got through equation (4) and equation (5).

III. PREDICTIONS CONSIDERING RESISTANCE LOAD

In order to verify the model and prediction method, single line and twisted-pair wires are lying in parallel in an experimental platform. They are bounded together with the length of 1 m and 30 mm high from the grounded plane. The cables are multi strand of copper wires with conductor cross sectional area 0.75 mm^2 , and their gauge is 227 IEC 06(RV). A series of rectangular pulses are used as an interference source to imitate the crystal oscillator signals. They have a frequency of 8 MHz, which is the frequency of the crystal oscillators used in electric control units (ECUs) in the experimental EV. Under this condition, 51 Ohm resistors are connected as terminal loads of both single line and twisted-pair wires.

A. Parameter measurement results

Short-circuit and open-circuit input impedances between different cables are measured by an impedance analyzer. The sweeping frequency is 0 Hz - 300 MHz. Part of the results are shown in Fig. 3 and Fig. 4. Where Z_{S11} is the short-circuit impedances between the single line and the reference plane; Z_{O11} is the open-circuit impedances between the single line and the reference plane; Z_{S12} is the short-circuit impedances between the single line and one of the twisted-pair wires; Z_{O12} is the open-circuit impedances between the single line and one of the twisted-pair wires.

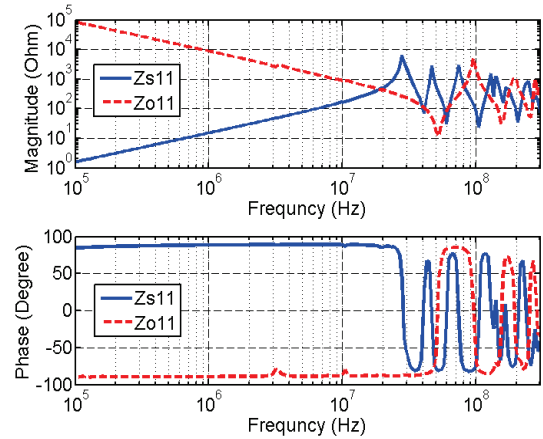


Fig. 3. Self-impedance measurement results of the single line.

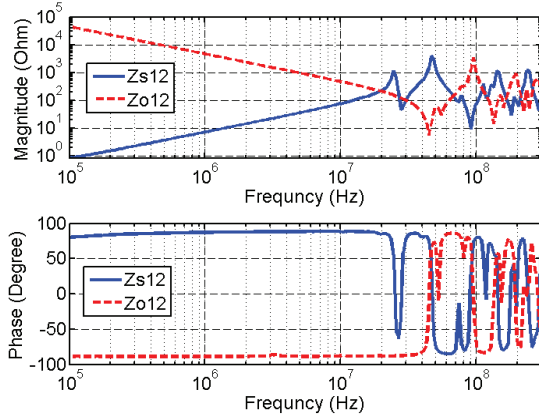


Fig. 4. Mutual-impedance measurement results between single line and one of twisted-pair wires.

Figures 3 and Fig. 4 suggest that, the open-circuit and short-circuit impedances change linearly in the low frequency range. While, there are oscillations in the high frequency range, because the inductances and capacitances of the crosstalk system are usually very small. These stray parameters will significantly affect the measured impedances among cables.

B. Predictions and experiments

Based on the parameter measurement results and the prediction algorithm, crosstalk spectrums can be predicted. In this paper, the terminal of twisted-pair wires close to the interference source is designated as the near terminal and the other is defined as the remote terminal. It is in consistent with the equivalent model in Fig. 1. Simulation study has been conducted in MATLAB in order to verify the performance of the proposed prediction method.

Considering 8 MHz pulse interference source, the predicted crosstalk spectrum of U_{t1} on the near terminal of twisted-pair wires is shown in Fig. 5, and the experimental result is given for comparison. In the same way, predicted spectrums and experimental results of U_{t2} on the remote terminal of twisted-pair wires are shown in Fig. 6.

Figure 7 shows the deviations between predicted and experimental spectrums for resistance loads. It suggests the predicted results have some differences with the experimental ones. Especially in a few frequencies, the deviation is bigger than 10 dBmV. This may be caused by the approximation of modeling process and measure deviations. However, average deviation in the whole frequency range up to 300 MHz is very small. Considering the main interference frequencies which have amplitudes higher than -65 dBmV, average deviation of the spectrum on the near terminal is 1.06 dBmV and average deviation of the spectrum on the remote terminal is 0.99 dBmV. Compared with the traditional crosstalk calculation method [18], deviations

of the proposed method are much smaller. So the proposed crosstalk predicted method has advantages in EV applications.

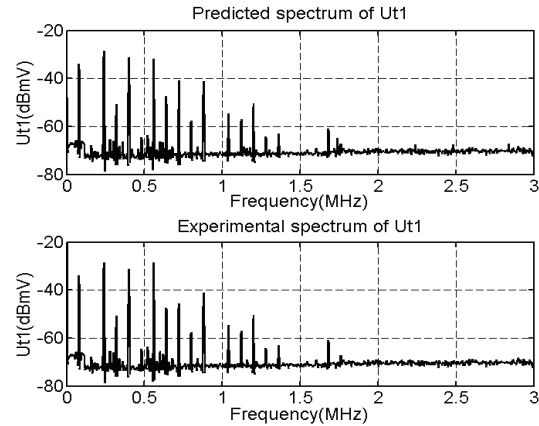


Fig. 5. Crosstalk spectrum predicted and experimental results on the near terminal for resistance loads.

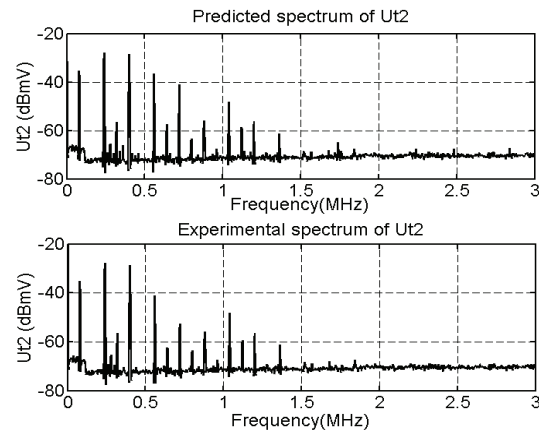


Fig. 6. Crosstalk spectrum predicted and experimental results on the remote terminal for resistance loads.

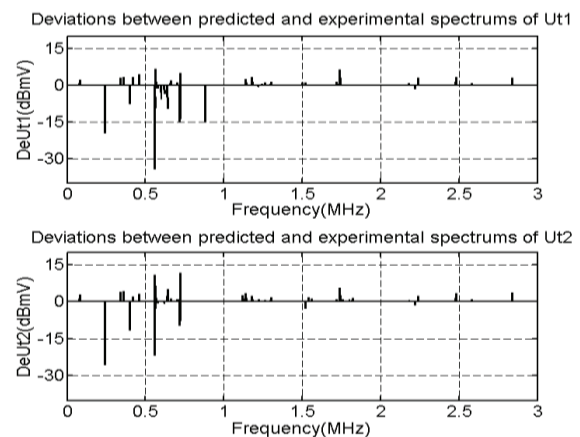


Fig. 7. Deviations between spectrum predicted and experimental results for resistance loads.

The predicted and experimental results not only prove the effectiveness of the method, but also provide materials for the frequency domain characteristics analysis of crosstalk in EV. They can be used to analyze the influence of the interference source. The interference source is a series of rectangular pulses, and the envelope curve of its spectrum is given by equation (9). Where A is the amplitude of the rectangular pulses, and τ is the width of the pulses:

$$F(j\omega) = A\tau \text{sinc}\left(\frac{\omega\tau}{2}\right) / \frac{\omega\tau}{2}. \quad (9)$$

So the amplitude of the interference source spectrum is decided by equation (9). The frequencies of the spectrum are the frequency of the pulses and its multiples. Figure 5 and Fig. 6 indicate that the interference frequencies of crosstalk voltages are basically the same as the source. However, there are some new interference frequencies appeared, which are caused by the non-linear factors, such as small deformations of the cables, non-uniform distances between cables and so on. Also, they have different amplitudes because of the influence of the frequency-dependent parameters. Besides, the amplitude of the crosstalk spectrum on the remote terminal is a little smaller than that on the near terminal. That is because the inductive coupling is positive on the near terminal but negative on the remote terminal as expressed in equation (4) and equation (5).

IV. PREDICTIONS CONSIDERING FREQUENCY-DEPENDENT LOAD

Many ECUs in EV have frequency-dependent characteristics. These ECUs are wildly used as loads of communication buses and their frequency-dependent impedances have effects on crosstalk interferences. So it is more appropriate to consider them for interference simulation and estimation.

Considering the experimental platform above, an ECU used for battery management system (BMS) in Fig. 8 is connected on the remote terminal of twisted-pair wires instead of the 51 Ohm resistor. The impedance is measured between the positive terminal and the negative terminal of the BMS without power. The measurement result is shown in Fig. 9.

The measured impedances can be described as a series of complex numbers, which change with frequencies. These complex numbers are used as $Z_{i2}(j\omega)$ in equation (4) and equation (5), so crosstalk spectrums can be calculated. Predicted and experimental results on the near and the remote terminal of twisted-pair wires are shown in Fig. 10 and Fig. 11. Also, the deviations between predicted and experimental spectrums for a frequency-dependent load are shown in Fig. 12.



Fig. 8. Photo of the battery management system.

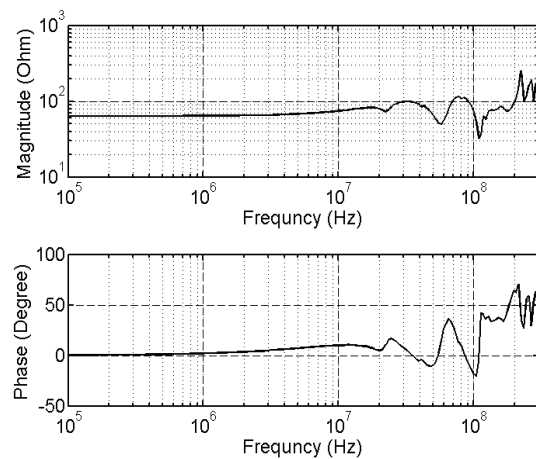


Fig. 9. Measurement impedance of the BMS.

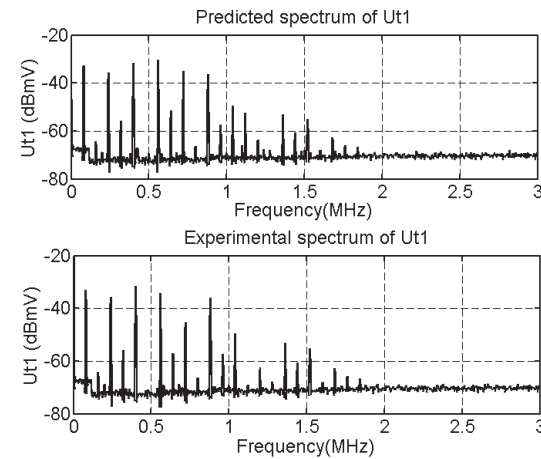


Fig. 10. Crosstalk spectrum predicted and experimental results on near terminal for a frequency-dependent load.

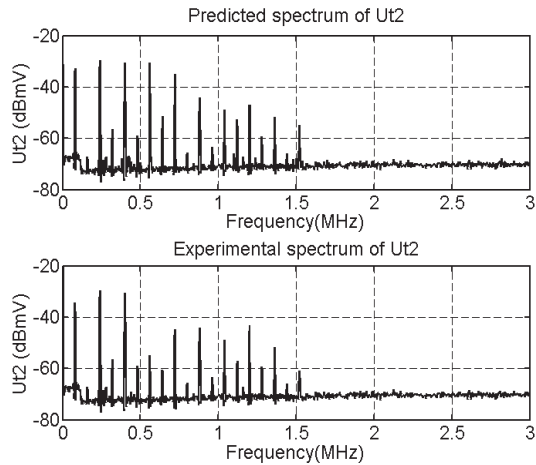


Fig. 11. Crosstalk spectrum predicted and experimental results on the remote terminal for a frequency-dependent load.

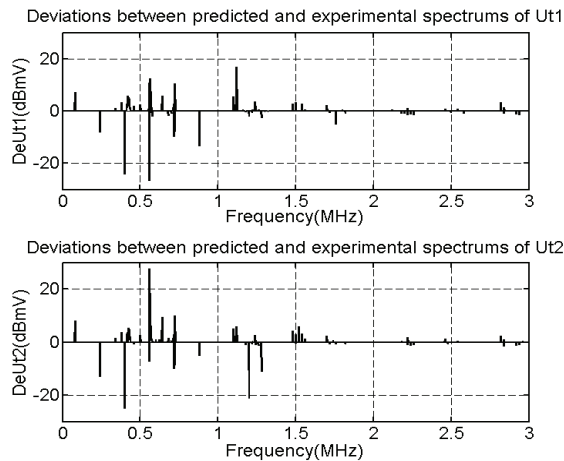


Fig. 12. Deviations between spectrum predicted and experimental results for a frequency-dependent load.

Similar with the results of resistance loads, predicted results have some differences with the experimental ones, especially in a few frequencies. However, considering the main interference frequencies which have amplitudes higher than -65 dBmV, average deviation of the spectrum on the near terminal is 1.92 dBmV, and average deviation of the spectrum on the remote terminal is 2.02 dBmV. Average deviation in the whole frequency range up to 300 MHz is also very small. So the proposed crosstalk prediction method is effective and has the advantage under the condition of frequency-dependent load.

These predicted and experimental results can be used to discuss the effects of the frequency-dependent load. The average deviations of a frequency-dependent load are only a little larger than the ones of resistance loads. It is caused by the following reason: Fig. 9 infers

that the impedance differences between a BMS and a 51 Ohm resistor are mostly in the high frequency range. In this range, amplitude of the interference source spectrum is even smaller than the background noises in the environment of electric vehicles. So the effects of BMS on the crosstalk spectrums are not very apparent as shown in Fig. 10 and Fig. 11. However, if the interference source has a higher frequency or the frequency-dependent loads have more complex inductive and capacitive impedances in the low frequency range, the effects will be significant.

So we believe that crosstalk spectrums are decided by the frequency characteristics of the interference source, the frequency-dependent parameters of the cables, and the terminal loads. Crosstalk spectrums can be predicted through the frequency-dependent parameter measurements, calculations, and the crosstalk equivalent model.

V. CONCLUSION

A simple method to predict crosstalk spectrums is discussed in this paper. It does not require long simulation time and substantial computing resources. Good accuracy has been achieved because frequency-dependent impedances of cables and terminal loads, which are obtained from measurements, are considered. So it is practical in some complex situations such as EV applications. This has been verified by experiments under the conditions of both resistance load and frequency-dependent load. The deviation analysis indicates the proposed method can provide more precise results than traditional crosstalk calculation method. Based on the simulations and experiments, the interference source, frequency-dependent parameters of cables and loads are analyzed to get the crosstalk frequency domain characteristics.

Although this method is proposed in the particular EV environment, it can be used in much more applications where conductors are put closely and their impedances can be measured easily. Also, this method will help interference suppression and electromagnetic compatibility (EMC) design.

REFERENCES

- [1] K. Prachumrasee, A. Siritariwat, and V. Ungvichian, "A methodology to identify crosstalk contributor from 6-line suspension assembly interconnect of ultra-high capacity hard disk drives," *Appl. Comput. Electromagn. Soc. J.*, vol. 27, no. 1, pp.22-27, Jan. 2012.
- [2] S. Weber, S. Guttowski, E. Hoene, *et al.*, "EMI coupling from automotive traction systems," *IEEE Int. Electromagn. Compat. Symp.*, Istanbul, Turkey, pp. 591-594, May, 2003.
- [3] M. Rajabi, and N. Komjani, "Improvement of transmission line matrix method algorithm

- frequency response based on modification of cell impedance,” *Appl. Comput. Electromagn. Soc. J.*, vol. 26, no. 4, pp.319-324, Apr. 2011.
- [4] M. Khodier, “Design and optimization of single, dual, and triple band transmission line matching transformers for frequency-dependent loads,” *Appl. Comput. Electromagn. Soc. J.*, vol. 24, no. 5, pp.446-452, Oct. 2009.
- [5] H. Jwaied, F. Muwanes, and N. Dib, “Analysis and design of quad-band four-section transmission line impedance transformer,” *Appl. Comput. Electromagn. Soc. J.*, vol. 22, no. 3, pp.381-387, Nov. 2007.
- [6] Y. W. Liu, D. S. Zhao, and K. K. Mei, “Implementation of generalized transmission-line equations to transmission line parameter extraction,” *Appl. Comput. Electromagn. Soc. J.*, vol. 18, no. 1, pp.58-64, Mar. 2003.
- [7] G. Ala, M. C. Di Piazza, G. Tine, *et al.*, “Evaluation of radiated EMI in 42-V vehicle electrical systems by FDTD simulation,” *IEEE Trans. Veh. Technol.*, vol. 56, no. 4, pp. 1477-1484, Jul. 2007.
- [8] O. M. Ramahi, “Analysis of conventional and novel delay lines: A numerical study,” *Appl. Comput. Electromagn. Soc. J.*, vol. 18, no. 3, pp.181-190, Nov. 2003.
- [9] K. Chamberlin, K. Komisarek, and K. Sivaprasad, “A method-of-moments solution to the twisted-pair transmission line,” *IEEE Trans. Electromagn. Compat.*, vol.37, no. 1, pp. 121-126, Feb. 1995.
- [10] X. P. Dong, H. X. Weng, D. G. Beetner, *et al.*, “A preliminary study of maximum system-level crosstalk at high frequencies for coupled transmission lines,” *IEEE Int. Electromagn. Compat. Symp.*, Silicon Valley, CA, pp. 419- 423, Aug. 2004.
- [11] W. T. Smith, C. R. Paul, and J. S. Savage*et c.*, “Crosstalk modeling for automotive harnesses,” *IEEE Int. Electromagn. Compat. Symp.*, Chicago, IL, pp. 447-452, Aug. 1994.
- [12] F. M. Ruan, S. Y. Sun, T. Dlugosz, *et al.*, “Some consideration on electromagnetic compatibility in CAN bus design of automobile,” *Asia-Pacific Int. Electromagn. Compat. Symp.*, Beijing, China, pp. 1431- 1434, Apr. 2010.
- [13] W. Li, S. F. Yu, B. Zhang, *et al.*, “High frequency conducted disturbance analysis of driving system in fuel cell vehicle,” *The 4th Asia-Pacific Environmental Electromagnetics Conf.*, Dalian, China, pp. 724-727, Aug. 2006.
- [14] C. Buccella, M. Feliziani, G. Manzi, *et al.*, “Prediction of voltage and current propagation in twisted wire pairs (TWPs) by a circuit model,” *IEEE Int. Electromagn. Compat. Symp.*, Chicago, IL, pp. 51-55, Aug. 2005.
- [15] W. R. Zimmerman, and L. D. Welles, “Measuring the transfer impedance and admittance of a cylindrical shield using a single triaxial or quadraxial fixture,” *IEEE Trans. Electromagn. Compat.*, vol.35, no. 4, pp.445-450, Nov. 1993.
- [16] B. Vanlandschoot, and L. Martens, “New method for measuring transfer impedance and transfer admittance of shields using a triaxial cell,” *IEEE Trans. Electromagn. Compat.*, vol.39, no. 2, pp.180-185, May. 1997.
- [17] S. Sali, “Cable shielding measurements at microwave frequencies,” *IEEE Trans. Electromagn. Compat.*, vol.46, no. 2, pp.178-188, May. 2004.
- [18] C. R. Paul, *Introduction to Electromagnetic Compatibility, 2nd ed.* Hoboken, NJ, John Wiley & Sons, Inc., 2006.



Yanjie Guo received the Ph.D degree in 2013 from Institute of Electrical Engineering, Chinese Academy of Sciences (IEECAS). Now he is an assistant professor in the Key Laboratory of Power Electronics and Electric Drive, Chinese Academy of Sciences. His research interest is mainly focus on electromagnetic compatibility (EMC), wireless power transfer, electric vehicles and power electronics.



Lifang Wang received the Ph.D degree in 1997 from Jilin University. She is currently the director of Department of Vehicle Energy System and Control Technology at IEECAS. She is also the vice director of Key Laboratory of Power Electronics and Electric Drive, Chinese Academy of Sciences. Her research interest is mainly focus on EMC, wireless power transfer, electric vehicles, vehicle control, power electronics, and power battery charging and management.



Chenglin Liao received the Ph.D. degree in 2001 from Beijing Institute of Technology and then spent 2 years as a postdoctoral researcher in Tsinghua University. Now he is a professor in the Key Laboratory of Power Electronics and Electric Drive, Chinese Academy of Sciences. His research interest is mainly focus on wireless power transfer, EMC, electric vehicles, and power battery.